CONTROLLING DIBLOCK COPOLYMER SELF-ASSEMBLY IN DIP-COATED THIN FILMS OF PS-P4VP WITH HYDROGEN-BONDING SMALL MOLECULES

Sébastien Roland, Christian Pellerin, Robert E. Prud'homme
and C. Geraldine Bazuin

Département de chimie, Centre de recherche sur les matériaux
auto-assemblés (CRMAA/CSACS), Université de Montréal,
C.P. 6128 succursale Centre-ville, Montréal (QC), Canada H3C 3J7

Introduction

Diblock copolymers are commonly used to create patterned surfaces at the nanometer scale, in view of their growing interest for applications, such as electronics,[1] optoelectronics,[2] biosensors,[3] nanolithography[4] and nanoreactors.[5] The immiscibility of the two blocks leads to characteristic morphologies that can be tuned by changing key parameters such as the Flory-Huggins interaction parameter for the two blocks, the degree of polymerization and the relative block fractions. In the case of block copolymer thin films, interfacial interactions, which often lead to preferential wetting of surfaces by one of the blocks, and film thickness, especially in relation to the natural periodicity of the block copolymer, additionally influence the film morphology.[6] In the present investigation, we use preferential interactions between functional small molecules (SMs) with one of the blocks of the diblock copolymer to further control the morphology of the thin films, following up on previous work on this subject.[5,7,8] Specifically, solutions of polystyrene-*b*-poly(4-vinylpyridine) (PS-P4VP) and naphthol (NOH) or naphthoic acid (NCOOH), both of which hydrogen bond to P4VP, were used to dip-coat solid substrates at various speeds and SM/VP molar ratios. Film surface morphologies were determined by AFM and the SM/VP molar ratios within the dip-coated films compared to that of the dipping solution were measured by infrared spectroscopy.

Experimental

Materials. The PS-P4VP diblock copolymer, with M_n = 41.5 kg.mol^{-1} for PS and 17.5 kg.mol^{-1} for P4VP (29.7 wt% P4VP), was purchased from Polymer Source, and used as received. 1-Naphthol (NOH, 98%), 2-naphthoic acid (NCOOH, 97%), and tetrahydrofuran (THF, 99.9%) were purchased from Aldrich, Fluka and VWR, respectively, and used as received. Silicon wafers ({1,0,0}) were purchased from University Wafer (Pittsburgh). Rectangular-shaped shards were cut (approximately 1 x 0.5 cm²) and cleaned by immersion in THF for at least 5 min, then wiped with a Kimwipe and dried under nitrogen flow.

Solution preparation. Solutions of 5 mg.mL^{-1} were prepared by dissolving 25 mg of block copolymer in 5 mL of THF. The desired small molecule at the desired SM/VP molar ratio was dissolved in the copolymer solution. The solutions were stirred overnight in closed vials on a heating plate at ca. 65 °C and then left to cool to ambient temperature. They were filtered twice, successively through 0.45 µm and 0.2 µm PTFE filters.

Film preparation. Films were prepared by dip-coating from the diblock copolymer/small molecule solutions at room temperature. The silicon substrates were vertically immersed in the solution at a rate of 5 mm.min^{-1}, followed by a pause of 30 s, then they were vertically withdrawn from the solution at a controlled rate using a KSV Langmuir film balance. The films were dried at ambient conditions in covered containers.

Fourier Transform Attenuated Total Reflection Infrared Spectroscopy (ATR). ATR infrared spectra, obtained from an accumulation of 256 interferograms at a resolution of 4 cm^{-1}, were recorded with a Tensor 27 Bruker Optics spectrometer equipped with a MCT (Mercury Cadmium Telluride) detector. A hemispherical Ge ATR crystal was used with p-polarized radiation at a 65° incident angle.

Atomic Force Microscopy (AFM). AFM images were obtained in tapping mode using a Multimode microscope controlled by a Nanoscope V controller (Veeco Instrument), operated under ambient atmosphere. The tips (Arrow-NCR, Al coated, spring constant 42 N/m, oscillation frequency ca. 285 kHz) were obtained from Nanoworld. Film thicknesses were determined from AFM images of scratches made with a scalpel.

Results and Discussion

It was previously reported that dip-coating from solutions of PS-P4VP mixed with NOH or NCOOH (SM/VP=1) under identical experimental conditions gives rise to different film morphologies: the quasi-hexagonal nodular or dot morphology is obtained from the NOH-containing solution and the fingerprint or stripe morphology from the NCOOH-containing solution.[8] Since then, additional experiments have shown that the behavior is more complex. As illustrated in Figure 1a-c, the dot morphology is observed in films of PS-P4VP/NOH (NOH/VP=1.0) for all of the dip-coating withdrawal rates used. In contrast, in films of PS-P4VP/NCOOH (NCOOH/VP=1.0), the stripe morphology is observed at high dip-coating rates (Fig. 1d) and the dot morphology at low dip-coating rates (Fig. 1f). A transition between the two morphologies can be observed at intermediate rates (Fig. 1e). It was verified by light scattering that there were no significant differences in the hydrodynamic radii for the NOH- versus NCOOH-containing systems in solution. In addition, it was observed that the film thickness decreases monotically with increase in dip-coating rate, from *ca.* 150 nm at the rate of 0.1 mm/min to a minimum of 7-10 nm for rates above *ca.* 5 mm/min.

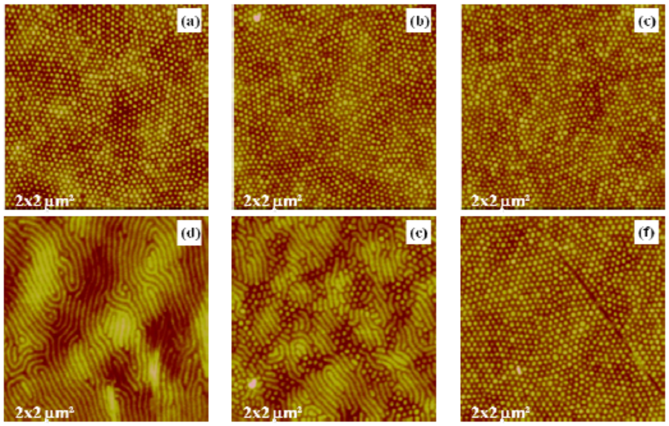

Figure 1. AFM height images of films made by dip-coating from THF solutions of PS-P4VP with equimolar (a-c) NOH, and (d-f) NCOOH at various withdrawal rates: (a,d) 2 mm/min, (b,e) 1.5 mm/min, and (c,f) 1 mm/min.

To help understand the morphological difference in the dip-coated films containing NOH and NCOOH, it may be useful to know if the proportion of small molecule taken up in the films compared to that in solution differs in the two systems. To determine this, infrared (IR) spectroscopy in the attenuated total reflectance (ATR) mode was used. Figures 2a (NOH) and 2b (NCOOH) exhibit the ATR-IR spectra of the dip-coated films obtained at different dip-coating rates. The spectra were normalized to the copolymer band at 1495 cm^{-1}, thus highlighting the change in intensity of the small molecule bands. Clearly, the intensity of the latter increases with dip-coating rate, qualitatively indicating that the SM/VP ratio in the films ("uptake ratio") increases with dip-coating rate. Consistent with this, there is a gradual shift in the band near 1600 cm^{-1} (composite band for the aromatic rings in P4VP, PS and NOH), from 1599 to 1601 cm^{-1} with increase in SM/VP ratio (insets of Fig. 2), reflecting an increase in SM hydrogen bonding to VP that shifts the pyridine part (and probably also the NOH part) of the band to higher wavenumbers.

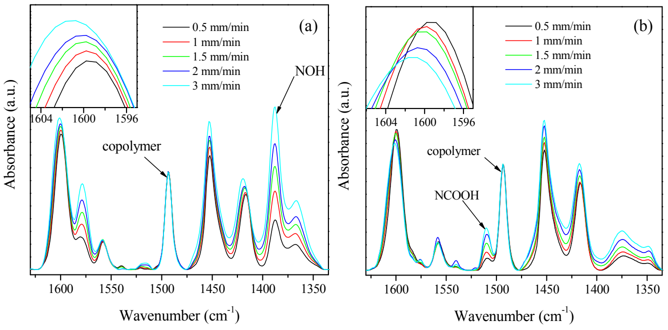

Figure 2. ATR-IR spectra of dip-coated films prepared at the specified withdrawal rates from (a) NOH- and (b) NCOOH-containing solutions (SM/VP=1.0). The spectra were normalized to the copolymer band at 1495 cm^{-1}. The inset shows a zoom of the band at *ca.* 1600 cm^{-1}, illustrating the shift related to hydrogen bonding.

The SM/VP uptake ratios were quantified using the bands at 1395 cm^{-1} for NOH and at 1510 cm^{-1} for NCOOH, along with calibration curves obtained from solution-cast films with known SM/VP ratios. The SM/VP uptake ratios are plotted as a function of dip-coating withdrawal rate in Figure 3. It is observed that the values for the uptake ratios as well as their evolution with the withdrawal rate are very similar for the two small molecules. Thus, it can be concluded that this issue by itself does not account for the morphological difference in the NOH- versus NCOOH-containing films. It is noteworthy that the evolution in SM/VP uptake ratio is quasi-linear at low dip-coating rates until ca. 3 mm/min, after which it tends towards and reaches the SM/VP solution ratio.

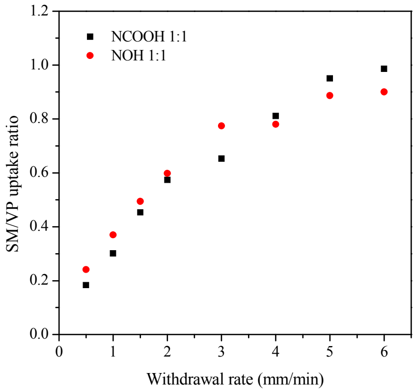

Figure 3. Small molecule/4-vinyl pyridine (SM/VP) uptake ratio as a function of the withdrawal rate in dip-coated films obtained from PS-P4VP copolymer solutions containing (●) NOH and (■) NCOOH in equimolar SM/VP ratio.

To further investigate the morphological evolution in dip-coated NCOOH-containing films, the NCOOH/VP solution ratio was varied to determine its influence, in conjunction with the dip-coating rate, on the NCOOH/VP uptake ratio and film morphology. For each solution composition, the NCOOH/VP uptake ratio increases with dip-coating rate, tending to a plateau corresponding to the NCOOH/VP solution ratio (as observed in Figure 3 for the equimolar solution). These curves collapse to a single curve when plotting uptake ratio/solution ratio *vs.* dip-coating rate. Since the dip-coating rate also determines the film thickness, the data obtained are shown in Figure 4 as a function of film thickness. This figure can be viewed as a pseudo-phase diagram where three main morphological areas can be distinguished, defined by lines A and B. The dot morphology only is observed below line A, and the stripe morphology only between lines A and B, with a narrow zone of the transitional morphology around A. Above line B, where the NCOOH in the films is in excess relative to VP, there is no regular pattern.

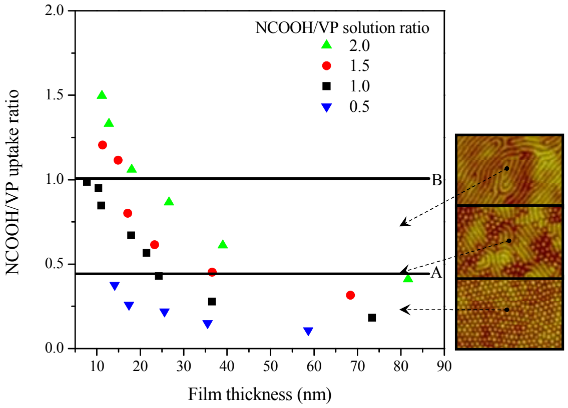

Figure 4. NCOOH/VP ratio in dip-coated films as a function of film thickness for dip-coating from PS-P4VP solutions containing the NCOOH/VP ratios indicated. The film morphologies observed are: the dot texture below line A, the stripe texture between lines A and B, and an irregular texture above line B. The transition between dot and stripe morphologies is observed in the vicinity of line A.

Figure 4 suggests that the film morphology in the PS-P4VP/NCOOH films is controlled essentially by the NCOOH/VP ratio in the dip-coated film. For well-defined surface morphologies (dot or stripe), the NCOOH/VP uptake ratio must not exceed equimolar. The stripe morphology is found for ratios between *ca.* 0.5 and equimolar and the dot morphology below *ca.* 0.45 NCOOH/VP ratio. On the other hand, the SM/VP uptake ratio in both NCOOH- and NOH-containing films depends on the dip-coating rate, and therefore, perhaps, on the film thickness. One possible explanation for this dependence is that the slower the withdrawal rate, the more time for the small molecule to diffuse from the depositing film back into solution during the dip-coating operation. Another possibility is that a surface-adsorbed or wetting layer[7, 9] closest to the substrate may contain the same composition as in solution, whereas the rest of the film contains much less. In this case, as the film thickness decreases to the order of the adsorbed layer thickness at the higher withdrawal rates, the composition observed in the film tends to the solution composition. It can also be speculated that the difference in hydrogen-bonding strengths between NCOOH (strong[10]) and NOH (intermediate strength[10]) to VP is somehow responsible for the difference in morphology behavior in the dip-coated films containing these two substances.

Conclusions

We have shown that self-assembling films dip-coated from THF solutions of PS-P4VP block copolymers mixed with NCOOH or NOH differ in morphology, depending on the nature of the hydrogen-bonding small molecule (perhaps via the H-bond strength) and, for NCOOH, on the SM/VP ratio in the film. The SM/VP ratio in the film, in turn, depends – independently of the nature of the small molecule – on the ratio in solution and on the dip-coating rate, which also determines the film thickness.

Acknowledgements. The research was funded by the Natural Sciences and Engineering Research Council of Canada (NSERC) and le Fond Québécois de la Recherche sur la Nature et les Technologies (FQRNT).

References

(1) Kim, H.-C.; Park, S.-M.; Hinsberg, W. D., *Chem. Rev.* **2009,** *110* (1), 146.

(2) Haberkorn, N.; Lechmann, M. C.; Sohn, B. H.; Char, K.; Gutmann, J. S.; Theato, P., *Macromol. Rapid Commun.* **2009,** *30* (14), 1146.

(3) Mistark, P. A.; Park, S.; Yalcin, S. E.; Lee, D. H.; Yavuzcetin, O.; Tuominen, M. T.; Russell, T. P.; Achermann, M., *ACS Nano* **2009,** *3* (12), 3987.

(4) Harrison, C.; Dagata, J. A.; Adamson, D. H.; Lithography with Self-Assembled Block Copolymer Domains, in: I.W. Hamley (Ed.), Developments in Block Copolymer Science and Technology, Wiley, Chichester, **2004,** 295.

(5) Kuila, B. K.; Nandan, B.; Bohme, M.; Janke, A.; Stamm, M., *Chem. Commun.* **2009,** (38), 5749.

(6) Ham, S.; Shin, C.; Kim, E.; Ryu, D. Y.; Jeong, U.; Russell, T. P.; Hawker, C. J., *Macromolecules* **2008,** *41* (17), 6431.

(7) Laforgue, A.; Bazuin, C. G.; Prud'homme, R. E., *Macromolecules* **2006,** *39* (19), 6473.

(8) Laforgue, A.; Gaspard, D.; Bazuin, C. G.; Prud'homme, R. E.; *Amer. Chem. Soc. Polym. Prepr.* **2007,** *48* (1), 670.

(9) Tokarev, I.; Krenek, R.; Burkov, Y.; Schmeisser, D.; Sidorenko, A.; Minko, S.; Stamm, M., *Macromolecules* **2005,** *38* (2), 507.

(10) Lee, J. Y.; Painter, P. C.; Coleman, M. M., *Macromolecules* **1988,** *21* (4), 954.